Molecular dynamics study of replica symmetry in the vulcanization transition

Sandra Barsky

Department of Physics and Astronomy, Johns Hopkins University, Baltimore, Maryland 21218

Michael Plischke

Physics Department, Simon Fraser University, Burnaby, British Columbia, Canada V5A 1S6

We report on computer simulations of the vulcanization transition of randomly crosslinked polymer melts. We focus on the order parameter between different realizations of the same distribution of random crosslinks, as well as the overlap distribution of these systems. [S1063-651X(99)17610-4]

I. INTRODUCTION

Vulcanization is a process by which a polymer melt is transformed from a liquid to an amorphous solid by the addition of crosslinks. Although this transition has attracted attention for many years, only recently have the techniques been developed to investigate some of the more interesting aspects of this problem. In particular, Goldbart and collaborators [1,2] have developed a replica theory of this transition and have made a number of specific predictions.

Crosslinks, which are randomly distributed throughout the melt, permanently join two monomers. These crosslinks do not necessarily constrain the connected monomers to a specific spatial location in the system, but rather the monomers must remain close to each other. The crosslinks are thus fixed along the arclength of the polymers, but not fixed in space. When the density of crosslinks exceeds some critical value, a fraction of the monomers becomes localized about mean positions and the melt solidifies. The critical crosslink density was estimated by theory and simulation to be $n_c \approx 1$ crosslinks per polymer.

The specification of the crosslink positions along the backbone of the polymers does not uniquely define the topology of the network. This can be seen by imagining a network of polymers where the crosslink points are well defined, but where there is no excluded volume restriction of the allowed configurations. All configurations consistent with the crosslink points are allowed; polymers can pass through one another and thus loops and entanglements can continually reform. If excluded volume is imposed on this system after a period of time, the polymer topology at that instant is frozen into the system. It is clear that had the excluded volume been imposed at a later time, the network would be frozen with a different topology. Thus, even with a given set of crosslink positions, the physical network has available to it a wide variety of topologies. Each of these systems with identical crosslink points but different topologies is known as a different replica of the same system. The introduction of a sufficient density of crosslinks, and the imposition of excluded volume, partitions phase space in a complex way. One level of partitioning is created by the crosslinks, where each of the regions created is ergodically explored by the network, in the absence of excluded volume. When physical dynamics is restored, each region is further

partitioned due to topological constraints. If the topological partitions, for a given crosslink realization, are related by translational symmetry, then there is a unique way for the system to solidify. In this instance, the excluded volume does not destroy the ergodicity of each crosslink realization. Otherwise, the excluded volume partitions phase space into disjoint regions not related by symmetry. There is then more than one way to solidify for a given realization of crosslinks, and replica symmetry is broken [2]. This possibility is the focus of the present work.

To measure the effect of topology we compare different replicas α, α' of a polymer system. The microscopic details of the two replicas are identical, i.e., the same monomers are linked, but differ in topological entanglements. The overlap $q^{\alpha\alpha'}$ is defined in the following way,

$$q^{\alpha\alpha'} = \frac{1}{\mathcal{N}} \sum_{j=1}^{\mathcal{N}} \langle e^{i\mathbf{k}\cdot\mathbf{r}_j^\alpha} \rangle \langle e^{-i\mathbf{k}\cdot\mathbf{r}_j^{\alpha'}} \rangle \tag{1}$$

where $\mathbf{r}_j^\alpha$ is the position of the jth monomer in the state α, the sum is over all the monomers in the system $\mathcal{N}$, and the angle brackets are a time average over a molecular dynamics (MD) run. When the two states coincide ($\alpha = \alpha'$) then $q^{\alpha\alpha}$ is the self-overlap or order parameter which differentiates the liquid from amorphous solid phases, which we have studied previously [3]. The theoretical predictions [1,2], confirmed by simulation, are $q^{\alpha\alpha} = 0$ in the liquid phase, and $q^{\alpha\alpha} > 0$ in the amorphous solid phase. Henceforth we concentrate on the latter case. When $\alpha \neq \alpha'$ there are two ways that the self-overlaps and the overlap can relate in the amorphous solid phase. Firstly, if $q^{\alpha\alpha} = q^{\alpha'\alpha'} = q^{\alpha\alpha'}$, then the two replicas are similar enough that the localized monomers fluctuate to the same extent about the same mean positions in each replica which means that the topological differences have no measurable effect. A second possibility is that $q^{\alpha\alpha} = q^{\alpha'\alpha'} \neq q^{\alpha\alpha'}$, in which case the two phases are *macroscopically* identical but *microscopically* different. Finally, if $q^{\alpha\alpha} \neq q^{\alpha'\alpha'}$ then the two replicas are in observably different macroscopic phases.

To better understand the role of the overlap, we introduce the probability distribution of the overlaps,

$$P(q) = \sum_{\alpha_1 \alpha_2} w_1 w_2 \delta(q - q^{\alpha_1 \alpha_2}) \qquad (2)$$

where the sum is over all states α_1, α_2 associated with a particular crosslink realization and w_i is the Boltzmann weight of state i. In the liquid phase, the distribution $P(q)$ is a delta function at the origin, as with the high-temperature paramagnetic phase of spin-glasses. In the amorphous solid phase there are two possibilities for the distribution of the overlap. Firstly, $P(q)$ may be a delta function at a non-zero value of q. This implies that all the states are related to each other by symmetry, and any differences which exist between the states are local and do not affect macroscopic quantities, such as the overlap. The second possibility is that $P(q)$ has non-zero weight at a variety of q, hence is not a single delta function distribution. In the latter case, there are equilibrium states which are not related by symmetry; there are a variety of ways to freeze, the system ceases to be ergodic and replica symmetry is broken. In a phantom network, Goldbart and Zippelius [4] found that the replica approach applied to vulcanization showed no replica symmetry breaking. As discussed above, one mechanism to break this symmetry is the inclusion of excluded volume.

In a continuing investigation of vulcanization by molecular dynamics (MD) simulation, this paper focuses on the replica nature of the transition. As with previous work, we start with an equilibrated polymer melt and create a fixed number of crosslinks, randomly distributed throughout the melt. To explore the role that topology plays, several copies of a polymer system with the same distribution of crosslinks but with different topologies (i.e., different replicas), are compared. The effect of the topologies on the order parameter q, as well as the overlap $q^{\alpha \alpha'}$ is calculated. Due to the quenched nature of the disorder it is important to average over as many possible realizations of crosslink distribution as possible. Since this requires a large amount of computer time, we restrict ourselves to rather small systems consisting of at most $M = 200$ polymers with $N = 10$ monomers or $M = 100$ polymer of length $N = 20$.

This paper is organized as follows. In Sec. II we review the simulation technique used in this work. Results and analyses are presented in Sec. III, and Sec. IV concludes with a discussion.

II. MODEL

The polymer model and simulation technique are the same as was used in previous work [3,5], and are based on a polymer model extensively used by Kremer, Grest and co-workers [6]. All particles in the system interact through a truncated Lennard-Jones potential

$$U_{LJ}(r_{ij}) = \begin{cases} 4\epsilon \left[\left(\dfrac{\sigma}{r_{ij}} \right)^{12} - \left(\dfrac{\sigma}{r_{ij}} \right)^6 + \dfrac{1}{4} \right] & r_{ij} < 2^{1/6}\sigma \\ 0 & r_{ij} \geq 2^{1/6}\sigma. \end{cases} \qquad (3)$$

Adjacent monomers on a chain are tethered to each other by the potential [7]

$$U_{nn}(r_{ij}) = \begin{cases} -\dfrac{1}{2} k R_0^2 \ln \left[1 - \left(\dfrac{r_{ij}}{R_0} \right)^2 \right] & r_{ij} < R_0 \\ \infty & r_{ij} \geq R_0, \end{cases} \qquad (4)$$

where $R_0 = 1.5\sigma$ and $k = 30\epsilon/\sigma^2$. With these parameters, chains can not pass through one another for reasonable values of the temperature.

Polymer melts were created and equilibrated by constant energy molecular dynamics, with a mean temperature $k_B T/\epsilon = 1$, and density $\rho\sigma^3 = 0.8$, where $\rho = NM/V$, with V the volume of the computational box. The equations of motion were integrated forward in time by a standard velocity Verlet algorithm [8], and periodic boundary conditions were used. For a given system, several different polymer melts were used. A second melt was created from the first by letting the system evolve for at least 4×10^5 integration steps, with each time step $\delta t = .01\sqrt{m\sigma^2/\epsilon}$.

Once the melt was obtained, a fixed number of crosslinks per polymer, n, was imposed by randomly selecting pairs of monomers within a distance of 1.25σ. If the monomers were not previously linked to each other a crosslink was created by imposing the potential (4). At this point four identical copies of the system were created, and the monomers were assigned different velocities in each copy. To change the topology, the parameter R_0 was increased from 1.5σ to 4.5σ, and the parameter k was lowered from 30ϵ to 0.7ϵ. This choice of parameters allows polymers to pass through one another with little cost in energy. Using the Brownian dynamics routine outlined in [3], the network was advanced for 10^4 integration steps. During this time, the maximum nearest neighbor distance increased from approximately 1.3σ to 4.1σ. This process ensured that the different copies could have different entanglements. The parameters R_0, k were then slowly returned to their original values, while the temperature was periodically quenched to zero. The different copies of the system were then in principle in different topological states.

With several copies of one crosslink realization in different replicas, the production runs commenced. The temperature of the system was increased to $k_B T/\epsilon = 5$, and the time step lowered to $\delta t = .004\sqrt{m\sigma^2/\epsilon}$, and the simulations were constant energy MD. As discussed in [5] the increased temperature decreases the amount of running time needed to attain equilibrium. The equations of motion were integrated forward in time for up to 3.6×10^6 time steps.

The calculation of the self-overlap is discussed in detail in [3] but is briefly reviewed here. For each of the monomers j in the system we calculate the time average of the quantity

$$q_{\mathbf{k}}^{\alpha\alpha}(j,t) = \frac{1}{t} \sum_{t'=1}^{t} e^{i\mathbf{k}\cdot\mathbf{r}_j(t')}, \qquad (5)$$

where $\mathbf{k} = \dfrac{2\pi}{L}(n_x, n_y, n_z)$, L is the length of a side of the cubic computational box and n_i are integers. Due to computational limitations, only the three smallest available $\mathbf{k}$ vectors were used, i.e., [(100), (010), (001)], and the results were averaged. As discussed in [3,5] a series of partial time-averages of the self-overlap was constructed

$$q^{\alpha\alpha}(n,t) = \frac{1}{3NM} \sum_{\mathbf{k}} \sum_{j} |q_{\mathbf{k}}^{\alpha\alpha}(j,t)|^2. \qquad (6)$$

The initial value of this function is $q^{\alpha\alpha}(n,1)=1$, but it decreases to its equilibrium value with increasing t. The extrapolated long time value of $q^{\alpha\alpha}(n,t=\infty)$ is found by fitting $q(n,t)$ to a function of the form $q^{\alpha\alpha}(n,t)=q_0+at^{-1/2}+bt^{-1}$.

The overlap between pairs of replicas is calculated by

$$q^{\alpha\alpha'}(t) = \frac{1}{3NM} \sum_{\mathbf{k}} \sum_{j} e^{i\mathbf{k}\cdot\mathbf{r}_j^{\alpha}(t)} e^{-i\mathbf{k}\cdot\mathbf{r}_j^{\alpha'}(t)}. \qquad (7)$$

The probability distribution of the overlap is defined as

$$P(q) = \frac{1}{t-t'+1} \sum_{t'}^{t} \delta(q-q^{\alpha\alpha'}(t')). \qquad (8)$$

At $t'=1$ the positions of the monomers in the two states are relatively correlated. After approximately 25000 integration steps the value of $q^{\alpha\alpha'}(t)$ attained an equilibrium value about which it fluctuated. The sum in (8) was only calculated after $q^{\alpha\alpha'}(t)$ reached this equilibrium. The calculation of this probability distribution is similar to the calculation of the probability distribution used in the investigation of replica symmetry in spin glasses [9,10].

One method to determine the ergodicity of a system has been developed by Thirumalai *et al.* [11]. These authors define an energy metric

$$d(t) = \frac{1}{\mathcal{N}} \sum_{j} [\epsilon_{\alpha,j}(t) - \epsilon_{\beta,j}(t)]^2, \qquad (9)$$

where

$$\epsilon_{\alpha,j}(t) = \frac{1}{t} \int_0^t dt' E_{\alpha,j}(t'), \qquad (10)$$

and $E_{\alpha,j}(t)$ is the total energy of particle j in state α at time t. In the work of Ref. [11], the states α,β differed by the initial configurations and velocities of the particles. It was found that the function $d(t)$ decreased rapidly to zero for a liquid phase, whereas for a glassy phase $d(t)$ attained a plateau, from which it decreased slowly. This plateau indicated the presence of energy barriers large enough to prevent the two systems from sampling the same region of phase space. For the present case it is straightforward to compare $d(t)$ for two different replicas α,α'.

III. RESULTS

We report results for two different crosslink densities imposed on each melt. The first crosslink density chosen was just above the critical density for the transition into the solid phase $n_1 \sim n_c = 1$; the second density was well above the transition, $n_2 > n_c$, so that the systems were deep in the solid phase. The value of the crosslink density varied with M and N, and based on previous results [3,5] it was chosen so that the values of the self-overlap $q^{\alpha\alpha} \approx 0.1, 0.3$ for n_1, n_2 respectively.

TABLE I. Estimates of self-overlap $q^{\alpha\alpha}$.

	n_1	n_2
$N=10$, $M=100$	0.12	0.34
$N=10$, $M=200$	0.09	0.28
$N=20$, $M=100$	0.05	0.34

We begin with results for the self-overlap. When the crosslink density is close to the transition the topology should have a greater role to play in the degree of localization, since two polymer clusters may be connected by a single loop in one replica while these clusters may be disconnected in another replica. Conversely, when there are sufficient crosslinks to ensure that the system is well into the solid phase, the value of the self-overlap is expected to be far less sensitive to the topology. As noted in previous work [3], the variation of $q^{\alpha\alpha}$ for different crosslink realizations is great. For this reason many different crosslink realizations are necessary. In this work, the systems with $M=10$ monomers per polymer had four to ten different realizations of crosslinks, and the system with $M=20$ monomers had at least five different crosslink realizations for each value of n. The crosslink densities chosen for n_1 and n_2 were for $N=10$, $M=100$, $n_1=1.15$, $n_2=1.5$; $N=10$, $M=200$, $n_1=1.03$, $n_2=1.3$; and for $N=20$, $M=100$, $n_1=1.05$, $n_2=1.60$. The average values of self-overlap are shown in Table I. The variation for the self-overlap is shown in Figs. 1(a) and 2(a) for $M=100$ polymers of length $N=10$, and in Figs. 1(b) and 2(b) for $M=200$ polymers of the same length. From these data we see that there is some variation in the extrapolated value of $q^{\alpha\alpha}$ for different replicas with the same crosslink realization. Near the critical crosslink density, the particular implementation of crosslinks (realization) has a greater effect on the value of the self-overlap than the different replicas of a given crosslink implementation. This can be seen by examining how both the replicas and the realizations affect the value of the self-overlap. The former gives information on how only topological connections affect $q^{\alpha\alpha}$ for a particular crosslink realization, while the latter gives information on the variation of $q^{\alpha\alpha}$ due to the many ways that crosslinks can be imposed on the system. To see how the topology affects the value of the self-overlap we examine the largest spread in self-overlap, $\Delta q^{\alpha\alpha}_{\text{replica}}$. For any one implementation of crosslinks the largest spread is $\Delta q^{\alpha\alpha}_{\text{replica}}=0.1$ in realizations 4 and 7 for $M=100$ polymers and in realization 4 for $M=200$ polymers, Figs. 1(a) and 1(b), respectively. At the higher crosslink density the spread in self-overlap for a given realization is still large at $\Delta q^{\alpha\alpha}_{\text{replica}}=0.12$ for $M=100$ and $\Delta q^{\alpha\alpha}_{\text{replica}}=0.08$ for $M=200$, Fig. 2. This large spread in the value of self-overlap for any given realization indicates that even well into the solid phase the value of $q^{\alpha\alpha}$ is highly dependent on the topological entanglements.

The theoretical model of Goldbart and Goldenfeld [1] raised the possibility that different replicas might be in different macroscopic phases, i.e., $q^{\alpha\alpha} \neq q^{\alpha'\alpha'}$. We note that in the terminology of Ref. [1] the only possibilities considered for the self-overlap were either $q^{\alpha\alpha}=0$ in the liquid state or $q^{\alpha\alpha}>0$ in the solid state. For the crosslink density close to the transition $n_1=1.03$ or 1.05 we find considerable variation
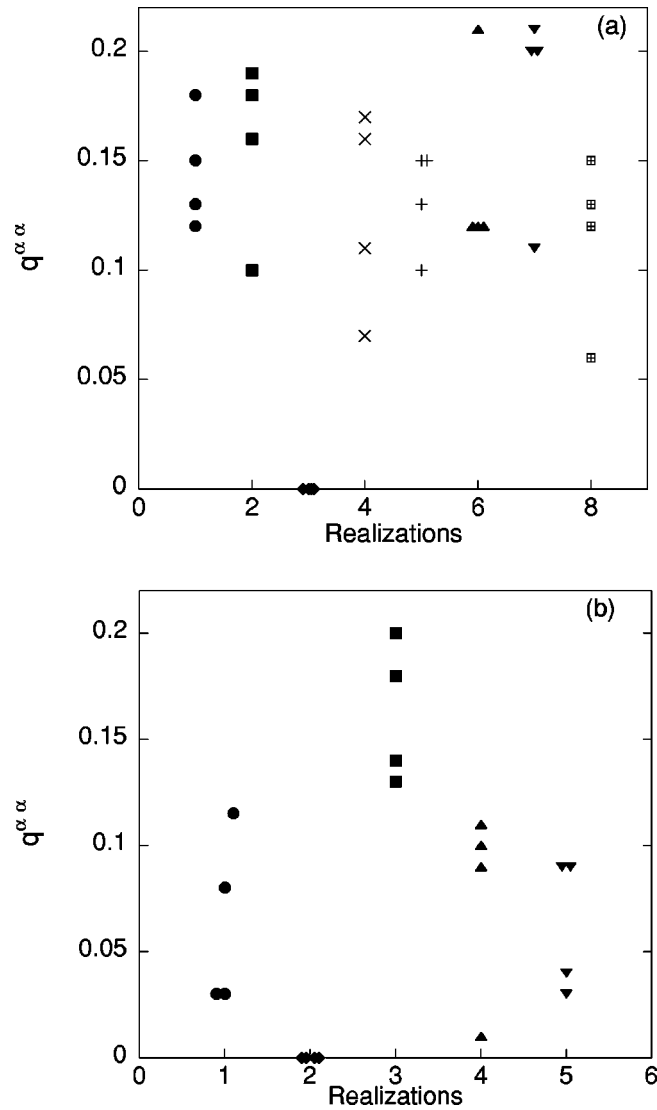
FIG. 1. Variation of the self-overlap $q^{\alpha\alpha}$ for different realizations of crosslinks at near the transition. Different symbols represent different implementations of the crosslinks (realizations). For a given crosslink realization the values of the $q^{\alpha\alpha}$ are plotted vertically for each of the four replicas. Part (a) is for the $N=10$, $M=100$ and $n_1=1.15$ system for 8 realizations. Part (b) shows the $N=10$, $M=200$ and $n_1=1.03$ system for 5 realizations. With crosslink density close to the transition density, there is a wide variation in value of self-overlap.

of the self-overlap but no evidence that some replicas are in the liquid phase whereas others are in the solid phase, for a given realization. That is, the extrapolated value of $q^{\alpha\alpha}$ for each replica with a *particular* crosslink distribution is either always equal to zero, or always greater than zero. As Fig. 1 shows, there is one realization in each of the $N=10$ systems where $q^{\alpha\alpha}=0$ for each replica, indicating that in those particular crosslink realizations, the crosslinks were distributed in such a way that these systems remained liquid. This situation occurs for crosslink densities near the transition and is a reflection of the random nature of the imposition of the crosslinks. The conclusion that all the replicas are in either the liquid or solid phase is based on relatively few crosslink realizations, and n_1 is still some distance from the transition point $n_c \approx 1$. Thus, these data do not eliminate the possibility
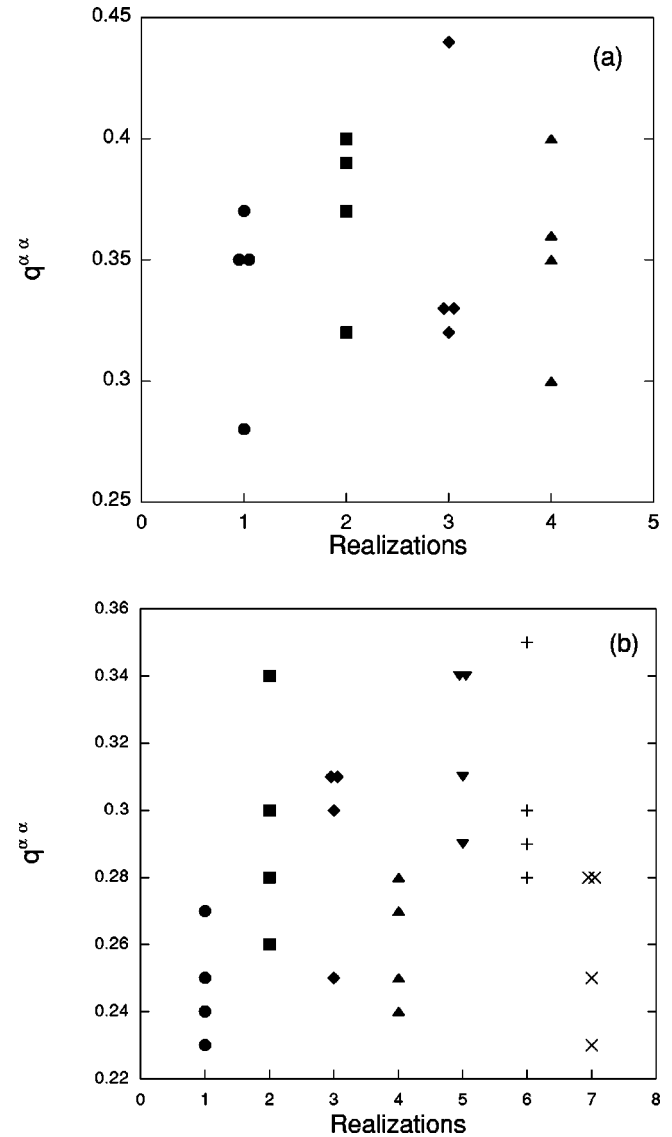
FIG. 2. Same as Fig. 1 but for crosslink density $n_2=1.3$. This crosslink density is farther into the solid phase.

that different replicas may be in different macroscopic phases, but this would occur much closer to the critical crosslink density.

The overlap probability distributions $P(q^{\alpha\alpha'})$ for n_1 and n_2 are shown in Figs. 3 and 4, for all three systems studied. For each system, the probability distributions plotted are the average of all overlaps taken pairwise of all four replicas for all the realizations. The probability distributions are peaked at about the value of the self-overlap, but with weight at a variety of different $q^{\alpha\alpha'}$ values. From these figures, we note that as the crosslink density increases, the distributions become narrower. With so few systems, finite size effects are difficult to establish, but we remark that the width of the distribution seems independent of system size. If the distributions became narrower with increasing system size, then one could conclude that as systems became larger the overlap distributions approach a delta function in the thermodynamic limit, indicating that replica symmetry is not broken. Since this is not the case, we conclude from this limited data set that the broad distribution of the overlap is not a finite
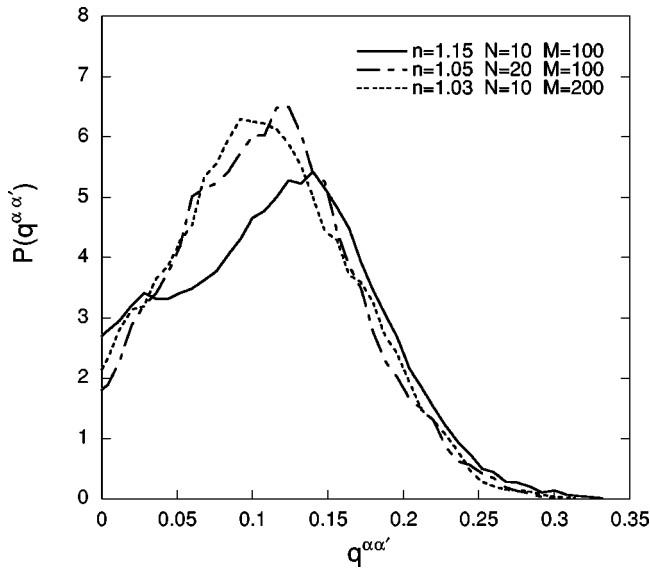
FIG. 3. The overlap distributions $P(q^{\alpha\alpha'})$ as a function of $q^{\alpha\alpha'}$ for all three systems studied at crosslink density $n_1 = 1.15$, 1.03, 1.05 for $N=10$, $M=100$, 200, $N=20$, $M=100$, respectively. The peak of the distribution approaches the value of the self-overlap as the systems increase in size but the width of the distribution stays large, indicating that the distributions remain broad with increasing system size.

size effect, hence that replica symmetry is indeed broken.

Another quantity of interest is the dependence of the value of self-overlap on the microscopic details of the crosslink realization. The dependence of the value of the order parameter on microscopic realization is related to the notion of self-averaging. If the variance of an observable quantity decreases to zero as a particular system increases in size, then that observable is self-averaging, otherwise the observable is non-self-averaging. Recently, Marinari *et al.* [12] argued that the signature of replica symmetry breaking was
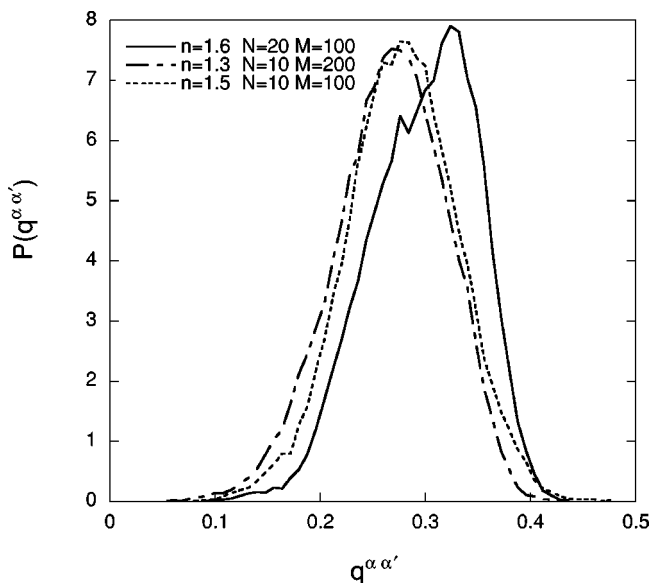

FIG. 4. The same as Fig. 3 for all three systems studied at crosslink density $n_2 = 1.5$, 1.3, 1.6 for $N=10$, $M=100$, 200, $N=20$, $M=100$, respectively.
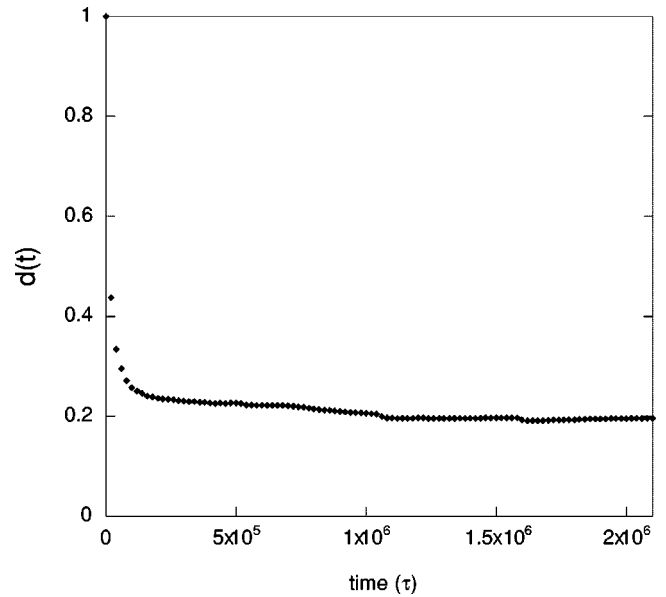

FIG. 5. The energy metric $d(t)$ reaches a plateau value for different replicas of a system of $N=10$, $M=200$ and $n_1=1.03$. This plateau indicates that there are energy barriers sufficient to prevent one replica from sampling the same phase space as another replica with the same realization of crosslinks.

the non-self-averaging of the order parameter. We compute the average value of the self-overlap of the four replicas of a particular realization, which is denoted by $q^{\alpha\alpha}(Re)$. For crosslink densities close to the transition, Fig. 1, $0 \leqslant q^{\alpha\alpha}(Re) \leqslant 0.18$ for $M=100$ and $0 \leqslant q^{\alpha\alpha}(Re) \leqslant 0.16$ for $M=200$, which is a significantly greater spread in self-overlap than $\Delta q^{\alpha\alpha}_{\text{replica}}$. The realizations close to the transition have a large variation in $q^{\alpha\alpha}$, as has been noted in previous work [3,5]. This dramatic variation in $q^{\alpha\alpha}$ is an effect of the imposition of the same number of crosslinks randomly in a given system. When more crosslinks are imposed on the system the averages of $q^{\alpha\alpha}(Re)$ for each realization are less varied, $0.34 \leqslant q^{\alpha\alpha}(Re) \leqslant 0.37$ for $M=100$ and $0.26 \leqslant q^{\alpha\alpha}(Re) \leqslant 0.32$ for $M=200$. By contrast the spread in the values of $q^{\alpha\alpha}_{\text{replica}}$ remain about the same as more crosslinks are imposed as noted above. In this more crosslinked case, the difference in self-overlap between the replicas of a given realization is larger than for different realizations. Although there are relatively few replicas and realizations of the system, there is little evidence for self-averaging, but conclusive proof awaits a larger study.

The different replicas necessarily mean that not every particle in one replica will access the same configuration space as its partner particle in a different replica. This means that phase space is partitioned into different regions which are not accessible by each replica of a given crosslink distribution. A measure of this broken ergodicity is found in Eq. (9). The energy metric is shown in Fig. 5. The states α, β of (9) are two different replicas of the same crosslink distribution. The function $d(t)$ decays rapidly to a relatively long-lived plateau value, from which it decreases slowly. Different pairs of replicas had different values of the plateau, which ranged from about 0.05 to 0.4. The kinks in the plateau were seen in a few but not all of the data sets, and likely correspond to rare events such as one or more polymers rearranging posi-

tion rapidly. There is no evidence that the plateaus decay to zero in the long time limit. Such behavior has been interpreted by the authors of [11] as evidence of broken ergodicity, something which we expect in this case. We note that if the two states α, β do not differ by topology, but by the velocity assigned to each particle the function $d(t)$ quickly decays to zero, and shows no evidence of a plateau [5]. This occurs even well into the solid phase.

IV. DISCUSSION

In a continuing investigation of vulcanization of polymers this work focused on the effect of topology on this transition. In this work we have investigated the replica nature of the vulcanization transition. For a given crosslink distribution the effect of topology on the self-overlap and overlap distribution was investigated. The self-overlap was measured using the order paramter $q(t)$ and was found to vary for different replicas, although this variation decreased as the density of crosslinks was increased. This result is consistent with the expectation that as more constraints are imposed on the polymers, the topological effects play less of a role in the determining the overall rigidity of the system.

The overlap distribution was measured by comparing the time averaged positions of monomers in different replicas. The distributions were found to be non-degenerate, indicating that different replicas are in non-symmetry related areas of phase space and that replica symmetry is broken. The data presented showed little finite-size effects, but the systems are relatively small with only a few replicas and crosslink realizations compared. Another test of replica symmetry breaking is the self-averaging of the order parameter. Although the systems studied here are quite small, there is no evidence that the order parameter self-averages. It remains to be seen if these results are upheld with larger system sizes.

[1] P. Goldbart and N. Goldenfeld, Phys. Rev. A **39**, 1402 (1989).
[2] See P.M. Goldbart, H.E. Castillo, and A. Zippelius, Adv. Phys. **45**, 393 (1996) for a recent review of this work.
[3] M. Plischke and S. Barsky, Phys. Rev. E **58**, 3347 (1998).
[4] P.M. Goldbart and A. Zippelius, J. Phys. A **27**, 6375 (1994).
[5] S. Barsky and M. Plischke, Phys. Rev. E **53**, 871 (1996).
[6] K. Kremer and G.S. Grest, J. Chem. Phys. **92**, 5057 (1990); **94**, 4103 (1991); J. Chem. Soc., Faraday Trans. **88**, 1707 (1992); E.R. Duering, K. Kremer, and G.S. Grest, Macromolecules **26**, 3241 (1993).
[7] R. B. Bird, R. C. Armstrong, and O. Hassager, *Dynamics of Polymeric Liquids* (Wiley, New York, 1977), Vol. 1.
[8] M. Allen and D. Tildesley, *Computer Simulations of Liquids* (Oxford University Press, Oxford, 1987).
[9] R.N. Bhatt and A.P. Young, Phys. Rev. B **37**, 5606 (1988).
[10] J.D. Reger, R.N. Bhatt, and A.P. Young, Phys. Rev. Lett. **64**, 1859 (1990).
[11] D. Thirumalai, R.D. Mountain, and T.R. Kirkpatrick, Phys. Rev. A **39**, 3563 (1989).
[12] E. Marinari, C. Naitza, F. Zuliani, G. Parisi, M. Picco, and F. Ritort, Phys. Rev. Lett. **81**, 1698 (1998).